Supplement of Atmos. Chem. Phys., 22, 13001–13012, 2022
https://doi.org/10.5194/acp-22-13001-2022-supplement

Supplement of

Source apportionment and evolution of N-containing aerosols at a rural cloud forest in Taiwan by isotope analysis

Ting-Yu Chen et al.

Correspondence to: Hui-Ming Hung (hmhung@ntu.edu.tw) and Haojia Ren (abbyren@ntu.edu.tw)

$\delta^{18}O$ variation in NO_3^- oxidation processes

The oxidation processes for aerosol NO_3^- formation can be represented as follows and shown as R1 to R10 in Fig. 1:

$NO + O_3 \longrightarrow NO_2 + O_2$ (R1)

$NO_2 + h\nu \longrightarrow NO + O$ (R2)

$O + O_2 \xrightarrow{M} O_3$ (R3)

OH radical oxidation:

$NO_2 + OH \xrightarrow{M} HNO_3$ (R4)

N_2O_5 hydrolysis at nighttime:

$NO_2 + O_3 \longrightarrow NO_3 + O_2$ (R5)

$NO_2 + NO_3 \xrightarrow{M} N_2O_5$ (R6)

$N_2O_5 + H_2O \longrightarrow 2HNO_3$ (R7)

OH formation:

$O_3 + h\nu \longrightarrow O + O_2$ (R8)

$O + H_2O \longrightarrow 2OH$ (R9)

peroxyl radical oxidation:

$NO + RO_2 \longrightarrow NO_2 + RO$ (R10)

If both oxygen atoms of NO_2 are from O_3 oxidation (R1), the O of NO_3^- would be 2/3 from O_3 and 1/3 from OH via OH oxidation (R4). On the other hand, if NO_3^- is formed via N_2O_5 hydrolysis during nighttime (R7), O atoms on NO_3^- would be 5/6 from O_3 and 1/6 from H_2O. Hastings et al. (2003) suggested that the $\delta^{18}O$ of OH radical was close to that of atmospheric H_2O (from -15‰ to 0‰ over the Asian continent, Global Network of Isotopes in Precipitation, IAEA); therefore, $\delta^{18}O$ of NO_3^- from OH oxidation (where $\delta^{18}O$ = +55‰ ~ +81.3‰) would be lower than that from N_2O_5 hydrolysis at night (where $\delta^{18}O$ = +72.5‰ ~ +101.67‰), as shown as yellow blocks in Fig. S6 and S7 (Hastings et al., 2003; Fang et al., 2011). However, if atmospheric OH radicals are mainly produced via R8 & R9, the $\delta^{18}O$ value of atmospheric OH could be the mean value of O_3 and H_2O in the range of +37.5‰ ~ +61.0‰ (half from O_3 and the other half from H_2O). The calculation would result in the same $\delta^{18}O$ (+72.5‰ ~ +101.67 ‰) of NO_3^- formed through the OH oxidation and N_2O_5 hydrolysis pathways.

If NO_2 has a significant contribution via the reaction of NO with peroxyl radicals (hydroperoxyl radical HO_2 or organic peroxyl radical RO_2) as R10, O atoms of HO_2 or RO_2 are supposed to have a similar $\delta^{18}O$ with atmospheric O_2 ($\delta^{18}O$ = +23.5‰, Luz and Barkan (2011)) as the O atom of the peroxyl radical is originated from atmospheric O_2 ($H + O_2 + M \rightarrow HO_2 + M$). Therefore, NO_2 from R10 reacting OH can produce NO_3^- with a lower $\delta^{18}O$ (could be low as +28.2‰ ~ +36.0‰) compared to that of NO_2 from R5 (+90‰ to +122‰). If the NO ↔ NO_2 cycle has rapidly exchanged through O_3 oxidation and NO_2 photolysis during the daytime, $\delta^{18}O$ of NO_2 would be close to that of O_3 after 7-8 times of reactions (Fig. S8). Therefore, $\delta^{18}O$ of formed NO_3^- would be +72.50-101.67‰ after either OH radical oxidation or nighttime N_2O_5 hydrolysis shown as

(P4) and (P6) in Fig. S6. If RO_2 radicals involve the oxidation processes, NO_3^- $\delta^{18}O$ could be low to +28.17‰ shown as (P7) in Fig. S7.

Isotope measurement details

All $\delta^{15}N$ and $\delta^{18}O$ have been analyzed at Ren's lab at Department of Geosciences, National Taiwan University, using 'denitrifier method'. We use denitrifying bacteria strains *Pseudomonas aureofaciens* for $\delta^{15}N$ and $\delta^{18}O$ analyses on nitrate samples, and *Pseudomonas chlororaphis* for $\delta^{15}N$ analyses on total N samples after oxidizing reduced N forms to nitrate. The analytical errors for $\delta^{15}N$ and $\delta^{18}O$ of nitrate samples are generally smaller than 0.1‰ using the 'denitrifier method' for samples containing 5 nmol N or more (Fig. S9). The errors become slightly bigger with smaller samples, e.g., at 2 nmol N. As a result, we have only analyzed samples with 5 nmol or more N. The linearity on the current setup is within 0.2‰ between 5nmol and 20nmol of N. But this does not affect our analyses, since we can correct for the linearity effect by analyzing samples and standards with constant N levels. Prior to isotopic analyses, we measure N concentration in each sample, so we could estimate the volume of samples needed to yield constant N amount (i.e., 5 nmol N). In addition, these samples are analyzed with standards at the same N level, such that any linearity effect will be sufficiently corrected. In addition, samples with very low nitrate concentration (less than 0.5 µmol/L in the dissolved solution) have greater errors for $\delta^{18}O$ analyses due to oxygen exchange effect with water during nitrate conversion. As a result, we only analyze samples that can yield greater than 1 µmol/L nitrate in the final dissolved solution. Samples or sample sizes will be binned if there is not sufficient N on each filter. Furthermore, we analyze samples with standards of similar concentration range. For example, samples with 7 µmol/L nitrate are analyzed with standards of 5 and 10 µmol/L nitrate, so the data correction using the nitrate standards also excludes uncertainties with different nitrate concentrations among samples. The above procedures are applied to all samples, which intend to address most if not all the uncertainties associated with isotopic analyses on nitrate samples. For total dissolved nitrogen, we use potassium persulfate reagent (3 g of Persulfate potassium and 5 g of Sodium hydroxide in 100 ml of Milli-Q water) to oxidize reduced N to nitrate prior to isotopic analyses. The main source of uncertainty in this oxidation step is associated with the blank of potassium persulfate reagent. We account for this uncertainty by using purified potassium persulfate after 3 times of recrystallization, which typically yield blank size of 0.4 µmol/L N, and account for 6% of the total oxidized sample on average. In addition, we also process 5 blanks and 3 to 4 oxidation standards using international standards USGS 40 ($\delta^{15}N$= -4.52 ‰) along with each run (typically containing less than 30 samples). The oxidation standards cover the range of blank/sample ratio in the samples, so we could also correct for blanks. Although we did not perform duplicates for the oxidation plus isotopic analyses on our samples, the 1 standard deviation for oxidation standards is less than 0.21 ‰, which represents the uncertainty for isotopic analyses for oxidized TN samples.

Table S1. Mass weighted isotope value (‰) of each group of samples.

	02D	**02N**	**13N**	**14D**	**14N**	**15D**	**20N**	**21D**	**22D**	**22N**
$\delta^{15}N$, NH_4^+	14.38	9.93	13.33	16.30	12.30	14.92	11.32	7.61	10.43	8.94
$\delta^{15}N$, PM_{1-10}-NO_3^-	2.72			3.70		4.24	1.85	5.20		
$\delta^{15}N$, PM_1-NO_3^-			1.46	1.50		1.93				
$\delta^{18}O$, PM_{1-10}-NO_3^-	70.05			70.75		72.45	74.82	72.52		
$\delta^{18}O$, PM_1-NO_3^-			79.81	69.07		72.01				
$\delta^{15}N$, NO_3^-	2.72		1.46	2.29		2.83	1.85	5.20		
$\delta^{18}O$, NO_3^-	70.05		79.81	69.67		72.18	74.82	72.52		

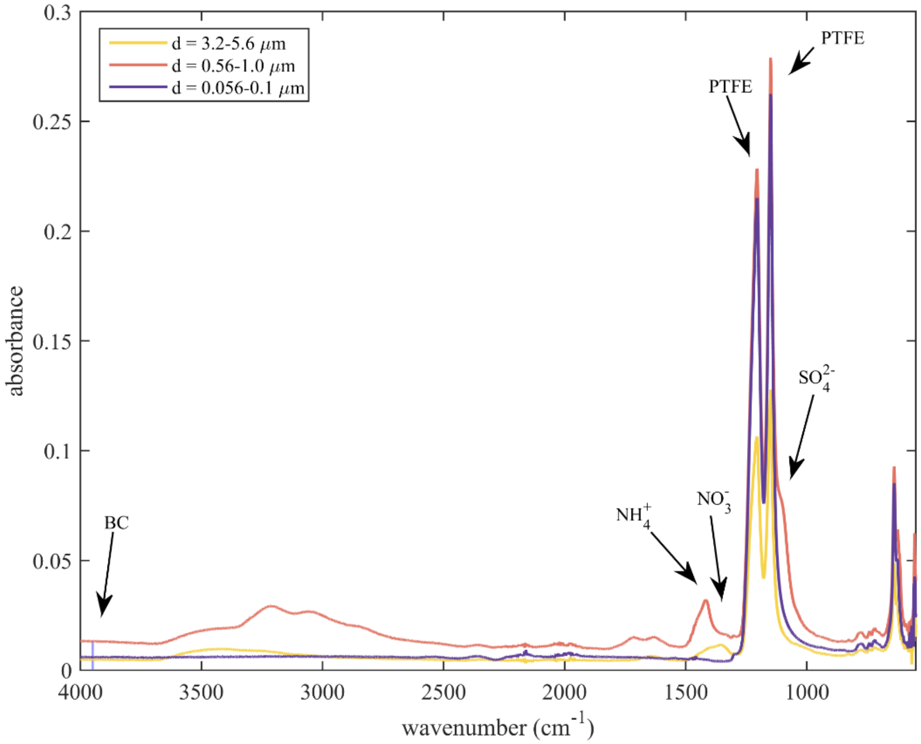

Figure S1. IR spectra of 3 collected samples on 2 December 2018. The absorption peaks for curve fitting are 2-curve fit for NH_4^+, NO_3^-; 3-curve fit for polytetrafluoroethylene (PTFE) and SO_4^{2-}; BC is determined using the average absolute absorbance of 3950 ± 5 cm^{-1} where have less interference by other chemical species.

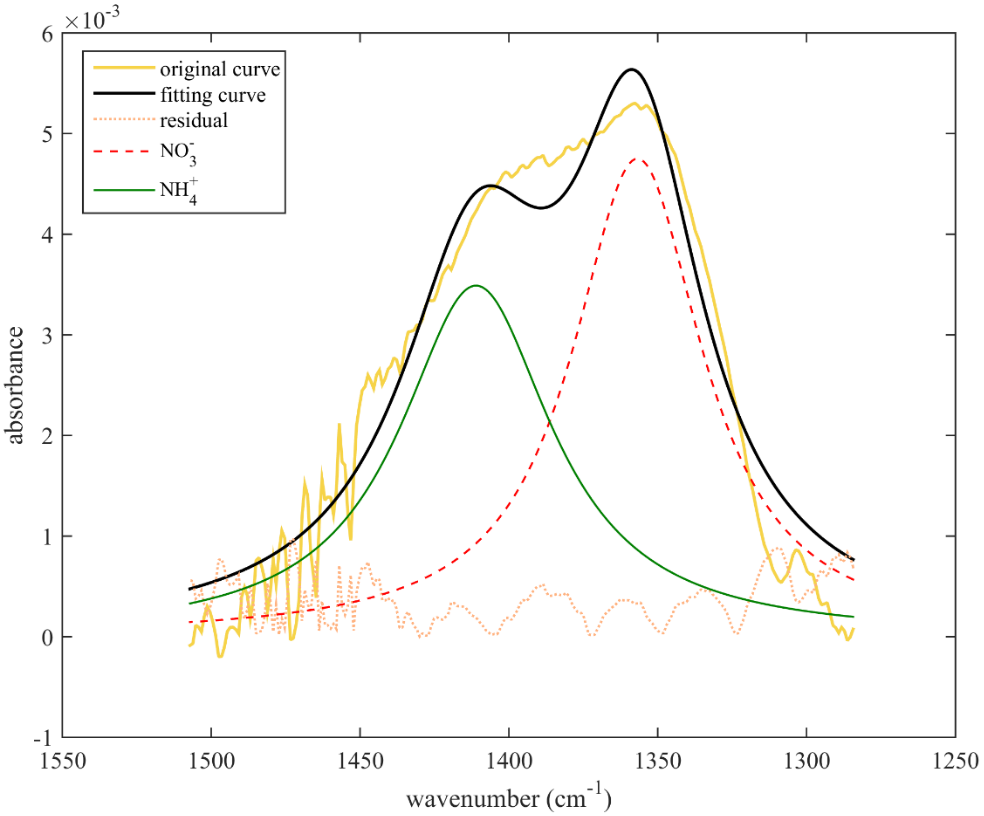

Figure S2. The Lorentzian fitting curve of the absorption curve of NH_4^+ and NO_3^-. The yellow thick curve is the background-corrected IR spectrum. Red and green curves are the fitted NH_4^+ and NO_3^- absorption curves, respectively. The black curve is the add-up of NH_4^+ and NO_3^- absorption, and the orange one represents the absolute value of the fitting curve minus the original curve.

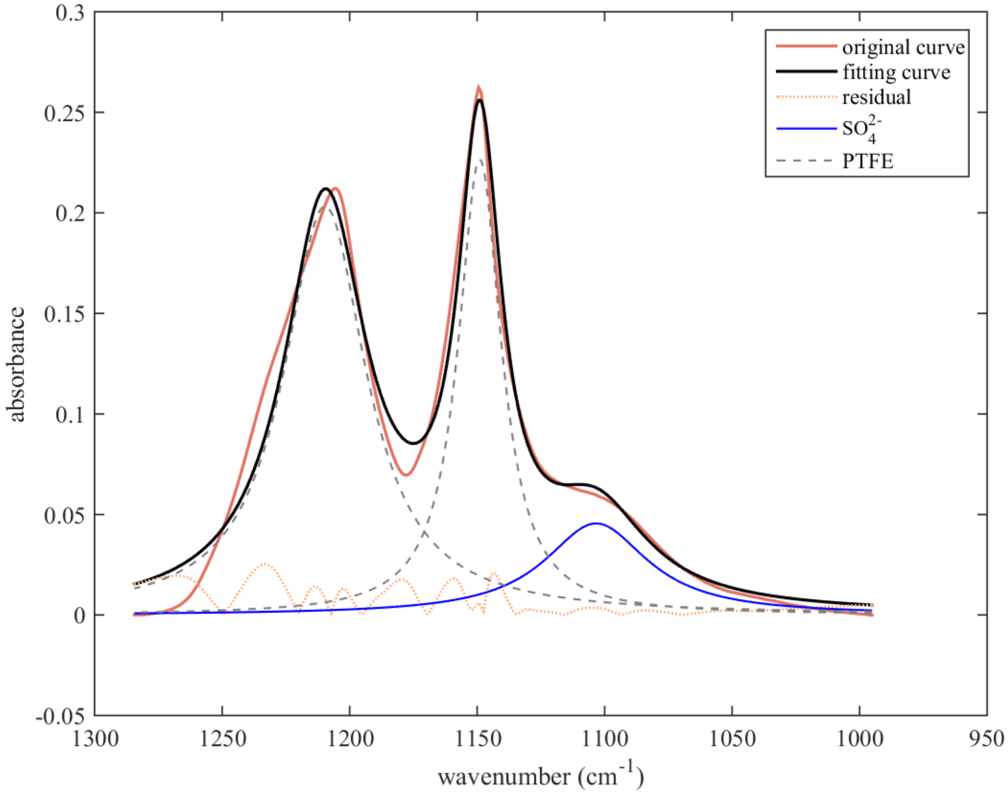

Figure S3. The Lorentzian fitting curve of the absorption curve of SO_4^{2-} and polytetrafluoroethylene (PTFE). The red curve is the baseline-corrected absorption curve. Two gray curves are the fitting curve of PTFE filter absorption, and the green line is that of SO_4^{2-}. The black thick curve is the add-up of absorption curves, and the orange one represents the absolute value of the fitting curve minus the original curve.

Concentration comparison between different methods

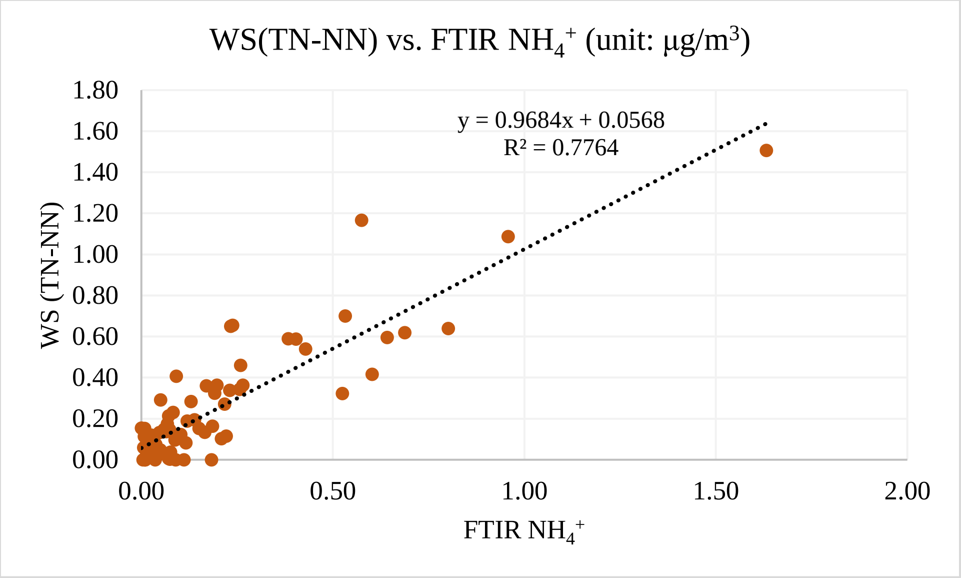

Figure S4. Comparison between the measured water-soluble (TN minus NN) and FTIR measured NH_4^+ concentration.

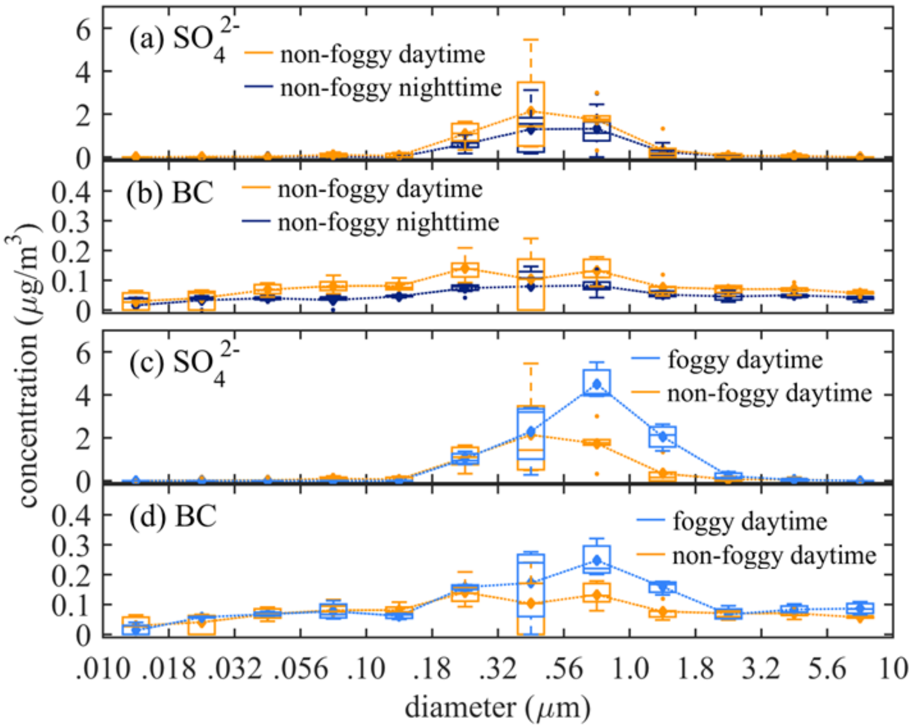

Figure S5. Statistic box plot of concentration of (A) SO$_4^{2-}$, (B) black carbon (BC) in non-foggy daytime and nighttime, and (C) SO$_4^{2-}$, (D) BC in the foggy and non-foggy daytime conditions in different cut-off sizes. (diamond: mean value; outliers: < 1st quartile Q1-1.5 interquartile range (IQR) or > 3rd quartile Q3+1.5 IQR).

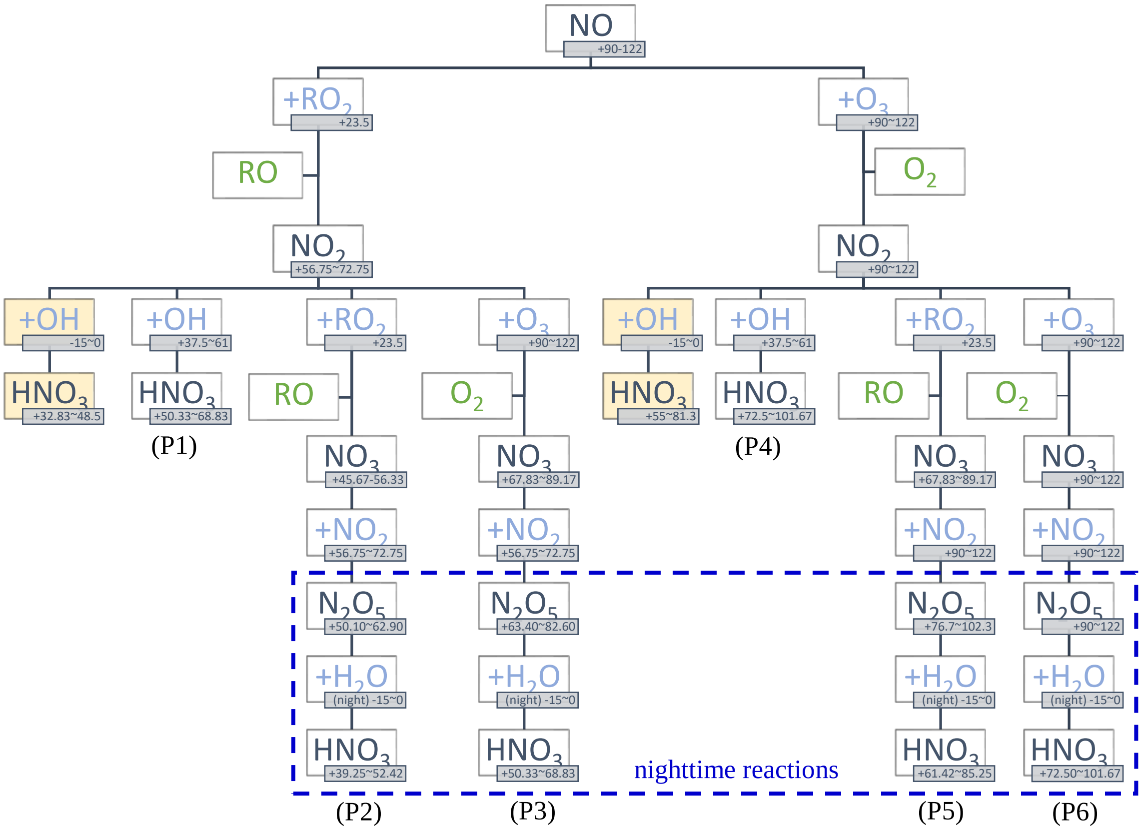

Figure S6. The predicted $\delta^{18}O$ (gray shaded bottom-right boxes) of products during HNO_3 formation pathways assuming the $\delta^{18}O$ of initial NO is 90~122‰ (i.e., fully reacted with O_3). Products are in dark-blue font color, reactants in light-blue, and by-products in green. The yellow-shaded boxes are based on the assumption of water-originated O atom of OH radical, whereas P1 and P4 have OH from the reaciton of $O(^1D)$ (generated from O_3 photolysis) with H_2O. The reactions in the dashed boxes are related to N_2O_5 hydrolysis occurring during nighttime.

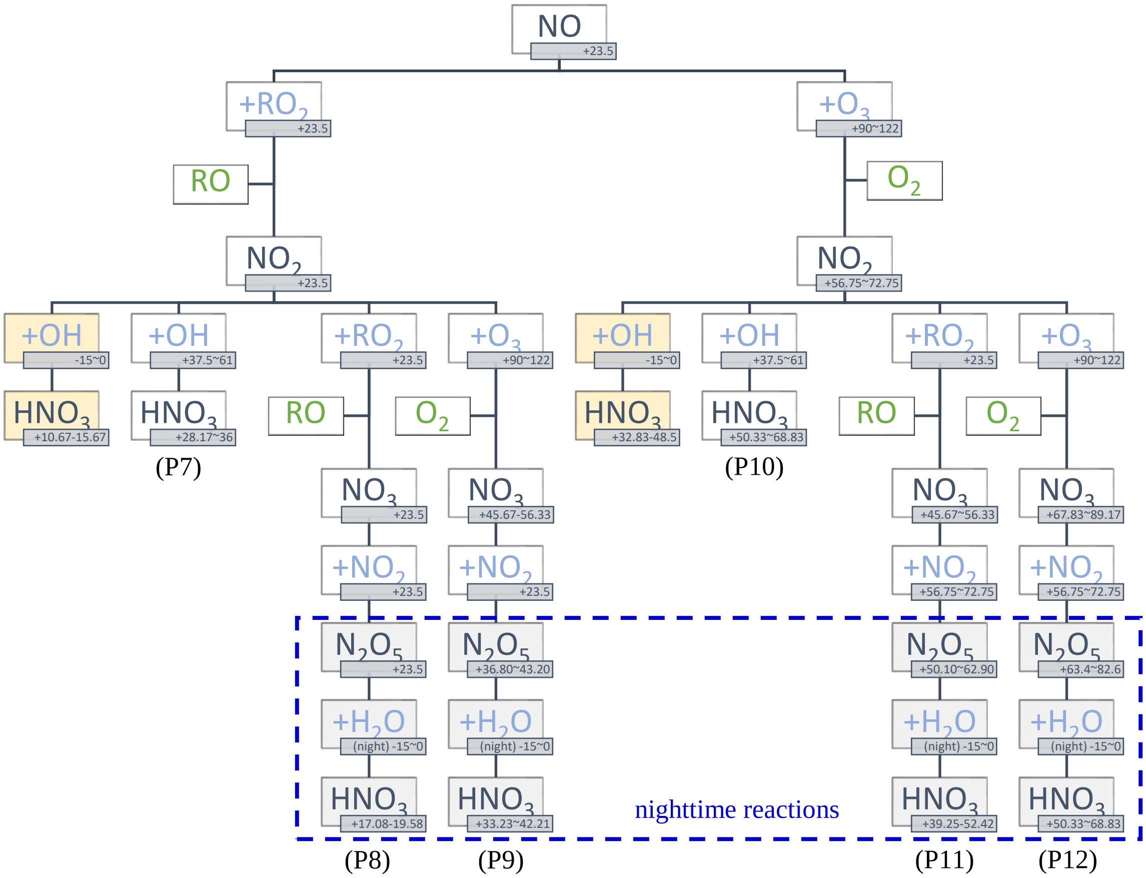

Figure S7. The predicted $\delta^{18}O$ (gray shaded bottom-right blocks) of products during HNO_3 formation pathways assuming the $\delta^{18}O$ of initial NO is +23.5‰ (i.e., freshly emitted and close to that of atmospheric O_2). Products are in dark-blue font color, reactants in light-blue, and by-products in green. The yellow-shaded blocks are based on the assumption of water-originated O atom of OH radical, whereas the O atoms of P7 and P10 are assuming that the OH is from O_3 and H_2O. The reactions in the dashed squares are related to N_2O_5 hydrolysis, where the reactions only occur at night.

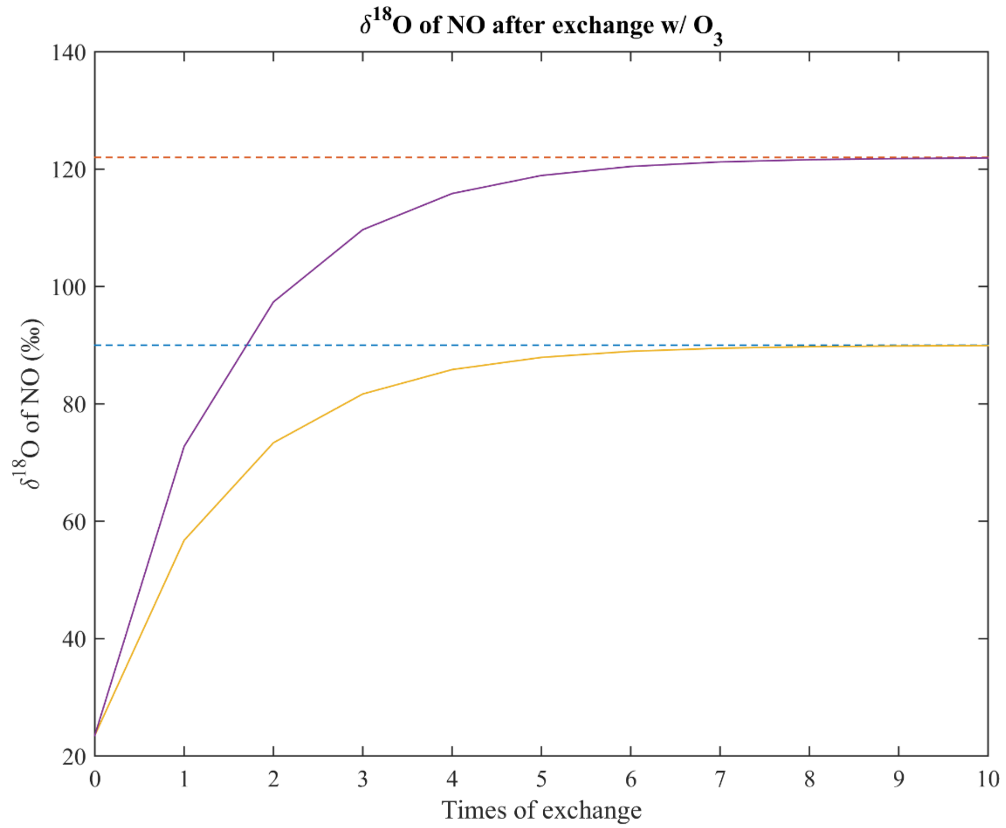

Figure S8. The predicted δ^{18}O of freshly formed NO (assume the δ^{18}O close of atmospheric O_2 = 23.5‰) after exchanging with O_3 (where δ^{18}O = 90~122‰).

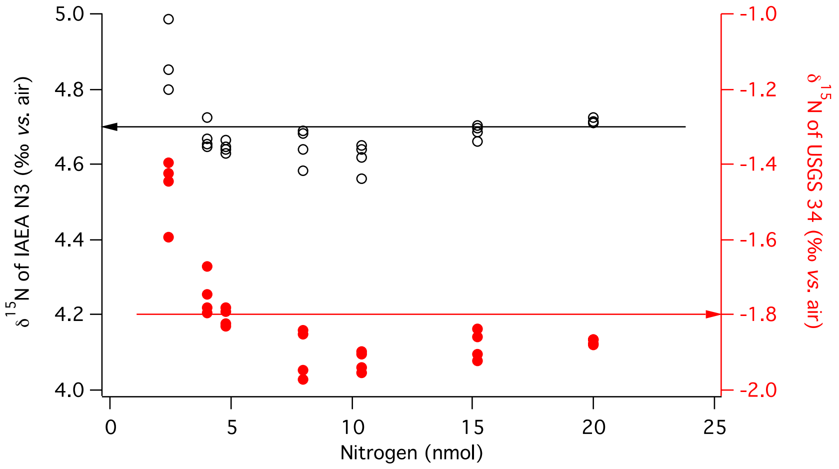

Figure S9. Measured $\delta^{15}N$ of IAEA N3 (open black circles) and USGS34 (closed red circles) at different nitrogen levels. The black and red lines indicate the true values of the two standards. One standard deviation of $\delta^{15}N$ at each nitrogen level is ~0.1 ‰. The changes in the measured $\delta^{15}N$ at different nitrogen levels reflect the current linearity of the system, which would be corrected with standards.

References

Fang, Y. T., Koba, K., Wang, X. M., Wen, D. Z., Li, J., Takebayashi, Y., Liu, X. Y., and Yoh, M.: Anthropogenic imprints on nitrogen and oxygen isotopic composition of precipitation nitrate in a nitrogen-polluted city in southern China, Atmospheric Chemistry and Physics, 11, 1313-1325, 10.5194/acp-11-1313-2011, 2011.

Hastings, M. G., Sigman, D. M., and Lipschultz, F.: Isotopic evidence for source changes of nitrate in rain at Bermuda, Journal of Geophysical Research: Atmospheres, 108, n/a-n/a, 10.1029/2003jd003789, 2003.

Luz, B. and Barkan, E.: The isotopic composition of atmospheric oxygen, Global Biogeochemical Cycles, 25, n/a-n/a, 10.1029/2010gb003883, 2011.